AWES2020
20th Australasian Wind Engineering Society Workshop
8 – 9 April, 2021

Coupling Numerical Weather Prediction Model and Computational Fluid Dynamics: Auckland Harbour Case Study

Amir A.S. Pirooz[1,2], Stuart Moore[3], Richard Turner[4], Richard G.J. Flay[5]
[1]*Meteorology and Remote Sensing, NIWA, Wellington, New Zealand.* amir.pirooz@niwa.co.nz
[2]*Department of Mechanical Engineering, University of Auckland, Auckland, New Zealand.*
[3] *Meteorology and Remote Sensing, NIWA, Wellington, New Zealand.* stuart.moore@niwa.co.nz
[4]*Meteorology and Remote Sensing, NIWA, Wellington, New Zealand.* richard.turner@niwa.co.nz
[5]*Department of Mechanical Engineering, University of Auckland, Auckland, New Zealand.* r.flay@auckland.ac.nz

ABSTRACT

As part of improving the resilience of large cities in New Zealand to extreme winds and tropical cyclones, this study investigates the feasibility of coupling the outputs of a very high-resolution, 333-m, numerical weather prediction (NWP) model with computational fluid dynamics (CFD) simulations. Following an extreme wind event on 18 September 2020 in Auckland, in which two trucks travelling over the Auckland Harbour rolled over damaging the bridge structure, here we conduct a CFD simulation of airflow over the bridge using the Reynolds-averaged Navier-Stokes (RANS) method and NWP wind speed forecasts as the inlet profile. The 333m NWP forecasts validated well compared to nearby observations, and CFD-based estimates of the wind speed-up over the bridge showed that the mean wind speed could increase by a factor of 1.15 – 1.20 in the vicinity of the road where the toppled vehicles were travelling. Also, gust estimations using mean wind speed and turbulence kinetic energy agreed well with measurements of the anemometer mounted at the top of the bridge arch.

1. Introduction

Rapid increases in urbanisation and population of cities as well as the design and construction of lighter and larger structures, necessitate a better understanding of the urban microclimate and associated hazards. This can lead to wind-resistant infrastructures and safer urban environments.

On 18th September 2020, a strong westerly wind in Auckland caused two trucks to roll over while heading south on the Auckland Harbour Bridge (yellow arrow in Figure 1), ultimately causing damage to the bridge's super structure (Stuff, 2018). Following this event, we defined the below research questions:

1- How accurately did NIWA's numerical weather prediction (NWP) model predicted this event?
2- What are the effects, i.e. wind speed-up, of the Auckland Harbour on the local airflow?

To address these questions, the study investigates the possibility of coupling the outputs of a high-resolution NWP with computational fluid dynamics (CFD) simulations.

The concept of coupling mesoscale models to a CFD model have been studied by several researchers, e.g. (Baik et al., 2009; Liu et al., 2012; Durán et al., 2020; and Piroozmand et al., 2020), to investigate various climate and environment parameters in urban areas, such as airflow, pollutant dispersion and air quality. A review of this coupling approach is provided by Kadaverugu et al. (2019). These works demonstrated that the approach is reliable and adds significant value to CFD simulations by downscaling the NWP models and using real events as input data to the CFD model. In this approach

both time varying and non-time varying boundary conditions provided by mesoscale models can be used as inlet conditions to the CFD model. For the present preliminary study, we use non-time varying boundary conditions for the CFD model obtained from a high-resolution NWP.

2. Methodology

The Auckland Model is based on the UK Met Office London Model (Boutle et al., 2016) and is a 333-m horizontal resolution convection-permitting configuration of the Unified Model (Boutle et al., 2016; Bush et al., 2020). The model set up is 300 x 300 grid-points, centred on the Auckland waterfront with a terrain-following 140 level vertical coordinate system over the lowest 40 km of the atmosphere. The Auckland Model is one-way nested inside NIWA's 4-km resolution NZLAM model, which is data-assimilating and uses the Global Atmosphere 6 science configuration (Walters et al., 2017) with an intermediate nest at 1.5 km resolution used to ease the transition from 4-km to 333-m resolution. The Auckland Model is run four times daily to two days ahead.

Figure 1 schematically shows the process of downscaling the 4-km NZLAM to 1.5-km model and lastly to the 333-m model. It should be noted that NZLAM4 domain is much larger than just over New Zealand. Figure 1 only shows part of NZLAM4 that covers New Zealand. Then the outputs of the downscaled model were used to setup the inlet profiles of the CFD model. As can be seen in Figure 1, the CFD model is only the isolated bridge model that has most of the main structures of the bridge and only very small details are removed. The computational domain extends 3 km from the centre of the bridge to the sides and 1.5 km to the top of the domain. Relatively fine mesh cells were generated around the bridge with a resolution of 4 m, and even finer down to 0.02 m around the smaller details of the bridge. The size of the cells gradually increases far from the bridge. Tetrahedral cells are used to ensure the complex geometry of the bridge is resolved. The total number of cells is about 32.7 million.

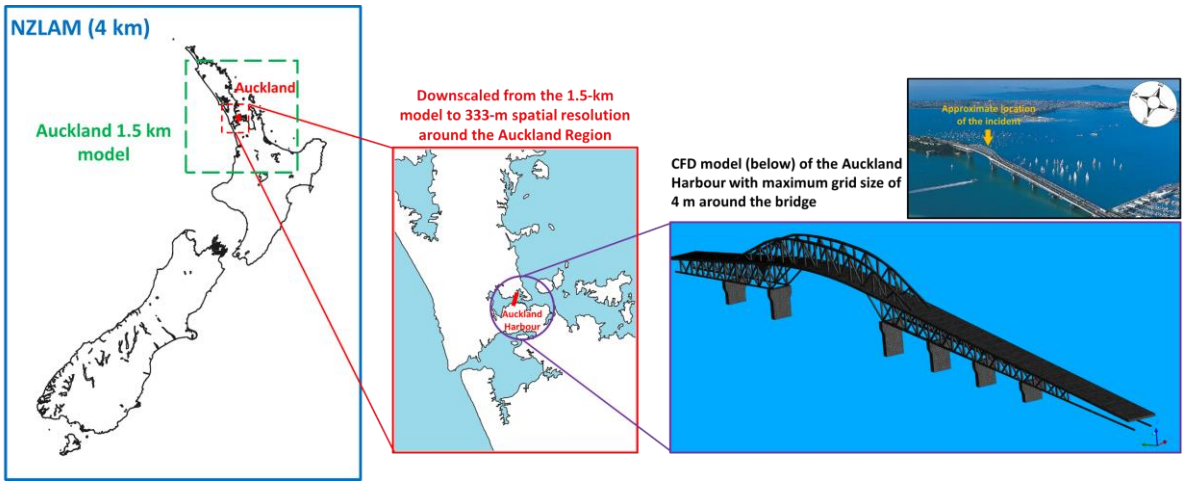

Figure 1. From left to right showing the process of the downscaling the 4-km NZLAM model to 1.5-km and to 333-m model around the Auckland region. The outputs of the 333-m are fed to a CFD simulation with 4-m grid resolution around the Auckland harbour bridge. Yellow arrow shows the approximate location of the incident.

For the event on 18 September 2020, mean and gust wind speed time series (Figure 2) were extracted from the relevant forecast cycle of the 333-m model. Figure 2a shows the model forecasts of the mean wind speeds at different vertical levels upstream of the Auckland Harbour. Since the Reynolds-averaged Navier-Stokes (RANS) approach is used in this study, which only provides time-averaged flow properties, the mean wind speed outputs of the 333-m were used to define the inlet profiles of the CFD simulation, as shown in Figure 3.

A pressure driven approach (Richards and Norris, 2015) was used to simulate the atmospheric boundary layer (ABL), utilising a three-dimensional, steady RANS simulation using the *k-w* Shear Stress

Transport (SST) turbulence model. The mean wind speed forecasts of the event shown in Figure 2a, were used to fit the velocity profile (Eq. 1, Figure 3a) and calculate friction velocity (u_*). It is shown in Figure 2a that the forecast mean speeds, and the fitted profile (Figure 3a), range from 11 m/s to 18 m/s at heights of 1 m and 103.7 m above the ground, respectively. Then, the corresponding profiles of the turbulent kinetic energy (k) and turbulent eddy frequency (ω) (Eqs. 2 and 3 and Figures 3b and 3c, respectively) were calculated. U, k, and ω profiles were set as the inlet boundary conditions of the computational domain. The symmetry boundary condition is used at the top boundary, the pressure-outlet boundary condition with zero-gauge pressure applied at the outlet of the domain, and for the ground, the automatic near-wall treatment was applied, replicating the sea roughness (z_0). For more details about the pressure-driven ABL, setting up the boundary conditions and resulting horizontally-homogenous computational domain see (Richards and Norris, 2015; Safaei Pirooz and Flay, 2018). It should be noted that the profiles in Figure 3 are only shown up to 140 m above the ground for a better visualisation of variables close to the ground. An example of full k profile extending to the top of the computational domain is shown in Figure 3b.

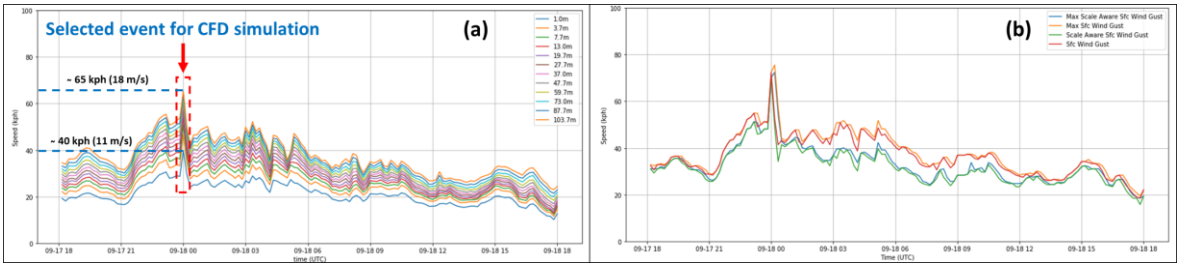

Figure 2. Mean (a) and gust (b) wind speed time series output of the 333-m model upstream the Auckland Harbour, during the extreme westerly event on 18 September 2020.

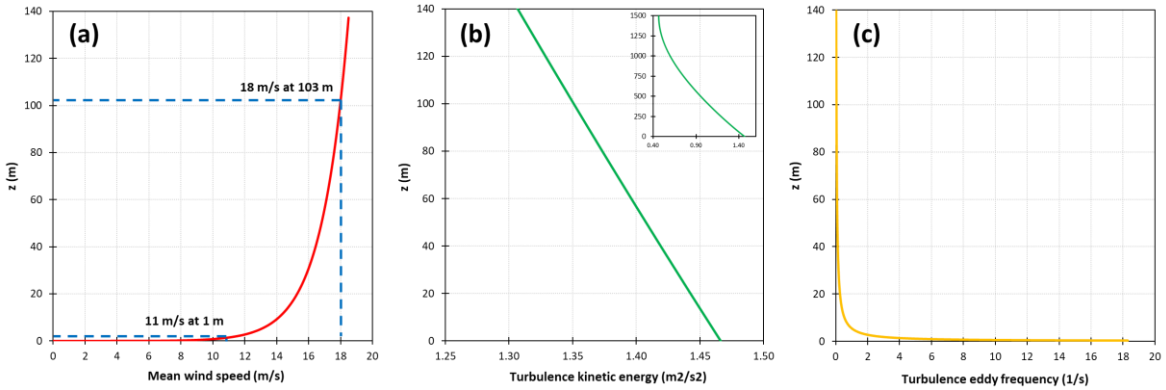

Figure 3. Inlet profiles for the CFD simulation: (a) mean speed; (b) turbulence kinetic energy. The smaller graph on top right shows the k profile extending to the top of the domain.; (c) turbulence eddy frequency.

$$U(z) = \frac{u_*}{\kappa}\left(\ln\left(\frac{z}{z_0}\right) + C_{U1}\left(\frac{z}{H}\right) + C_{U2}\left(\frac{z}{H}\right)^2 + C_{U3}\left(\frac{z}{H}\right)^3 + C_{U4}\left(\frac{z}{H}\right)^4\right), \quad (1)$$

$$k(z) = {u_*}^2\left(C_{k1} + C_{k2}\left(1 - \frac{z}{H}\right)^2 + C_{k3}\left(1 - \frac{z}{H}\right)^4 + C_{k4}\left(1 - \frac{z}{H}\right)^6\right), \quad (2)$$

$$\omega(z) = \frac{k(z)}{\kappa u_* z}\left(1 + (1 + C_{U1})\left(\frac{z}{H}\right) + (1 + C_{U1} + 2C_{U2})\left(\frac{z}{H}\right)^2 + (1 + C_{U1} + 2C_{U2} + 3C_{U3})\left(\frac{z}{H}\right)^3\right). \quad (3)$$

The CFD results using RANS equations present the mean flow variables. However, knowing the values of gust wind speeds is of great importance in studying wind hazards. Thus, to obtain the gust wind speeds (U_{gust}, Eq. 6), the standard deviation (σ_u, Eq. 5) needs to be approximated using the mean wind speed and turbulent kinetic energy. Popiolek (2008) demonstrated that the mean velocity and turbulent kinetic energy obtained from the RANS equations can be utilised to estimate a modified mean wind speed ($\overline{W_e}$, Eq. 4) and σ_u.

$$\overline{W_e} = \begin{cases} \overline{U} - 0.036k^{0.5} + 0.797\dfrac{k}{\overline{U}} - 0.179\dfrac{k^{1.5}}{\overline{U}^2} & if \quad \dfrac{k^{0.5}}{\overline{U}} < 1.592 \\ 0.287\overline{U} + 1.226k^{0.5} & if \quad \dfrac{k^{0.5}}{\overline{U}} \geq 1.592 \end{cases} \tag{4}$$

$$\sigma_u = \overline{U}^2 - \overline{W_e}^2 + 2k \tag{5}$$

Using the standard deviation and mean speed values, and that the wind velocity has a Gaussian probability distribution, the gust wind speed can be approximated by Eq. 6 (Holmes, 2015),

$$U_{gust} = \overline{W_e} + \mathrm{g}\sigma_u \ , \tag{6}$$

where g is a peak factor, whose value depends on the effective gust duration and often ranges from 3 (high gust duration, e.g. 3 s) to 3.4 (low gust duration, e.g. 0.2 s) (Safaei Pirooz et al., 2020).

3. Results and Discussion

Velocity streamlines of the westerly event on 18 September 2020 passing through the Auckland Harbour bridge are shown in Figure 4a, depicting wind speed-ups on the edge of the road as well as between the struts of the bridge. Figure 4b depicts the mean speed on a plane at the centre of the bridge along the road. The locations of high (red) and low (blue) wind speeds can be seen. Sheltering effects of the bridge components results in lower wind speeds.

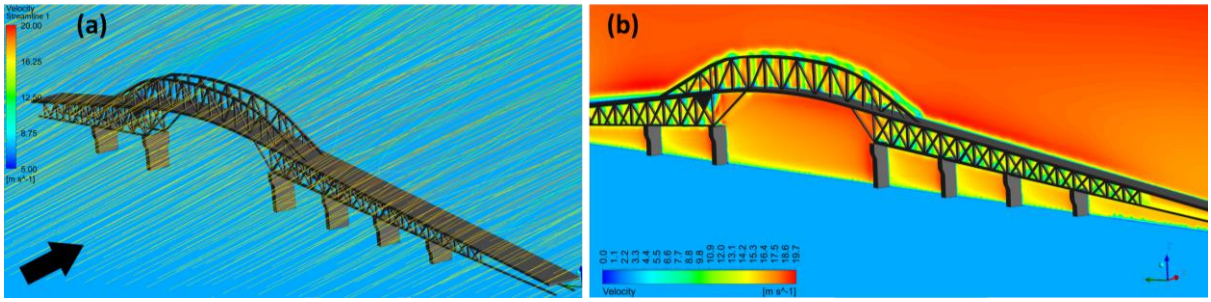

Figure 4. Overall airflow behaviour around the harbour for the westerly wind: (a) velocity streamlines; (b) contour of mean speed at the centre of the harbour.

To better realise the flow pattern across the width of the bridge, Figures 5a and 5b shows the mean wind speed and wind speed-ups, due to the presence of the bridge structure, respectively. The wind speed-up is defined as the wind speed at a specific location and elevation divided by the undisturbed upstream wind speed at the same elevation. It can be seen in Figure 5b that the mean speed can be increased by up to 1.15 – 1.20 in the middle of the bridge where vehicles travel. It is also noteworthy that the wake created by the bridge extends far downstream of the bridge.

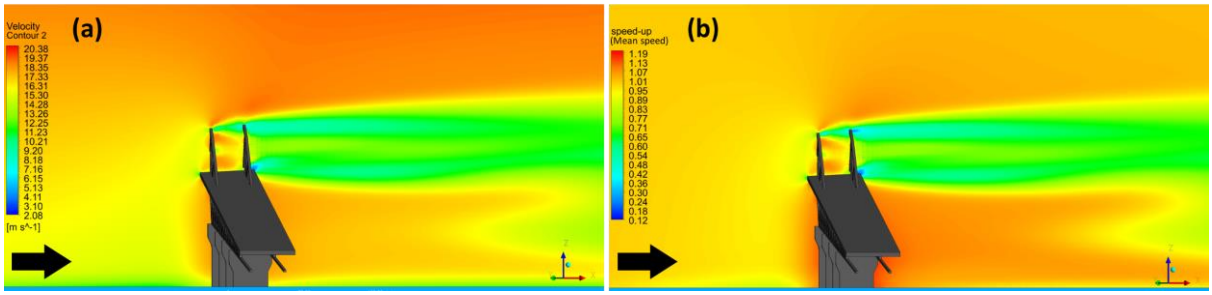

Figure 5. (a) mean speed and (b) mean speed-up values on a cross-sectional plane along the width of the bridge.

Gust wind speeds across the bridge estimated using mean wind speed and turbulence kinetic energy (Eqs. 4 – 6) are shown in Figure 6. The gust wind speeds reach around 22 – 24 m/s close to the surface

of road and flow separation is observed from the top arch of the bridge with high gust wind speeds of about 25 – 30 m/s. Through a personal communication with "Total Bridge Services" operating the Auckland Harbour, it was confirmed that there is an anemometer at the top of the arch that recorded a maximum gust of 127 km/h = 35.3 m/s during the event on 18 September 2020. It is clear from Figure 6 that the region above the top arch is affected by flow separation and has higher gust wind speeds. Therefore, measurements in the flow separation region may not reflect the real upstream wind speed, nor captured rightly by the 333-m NWP model (Figure 2b), due to the resolution of the NWP model, which does not see the finer structures and localised wind speed-ups.

In Figure 2a it was shown that at a hight of 103.7 m the forecast mean speed was 18 m/s. The bridge has a clearance hight of about 43 m (water to road). Figure 7 illustrates velocity iso-surfaces showing locations where the wind speed is 18 m/s. It is evident that the structure of the bridge affects the upstream airflow such that a mean wind speed of 18 m/s is predicted on the road of the bridge.

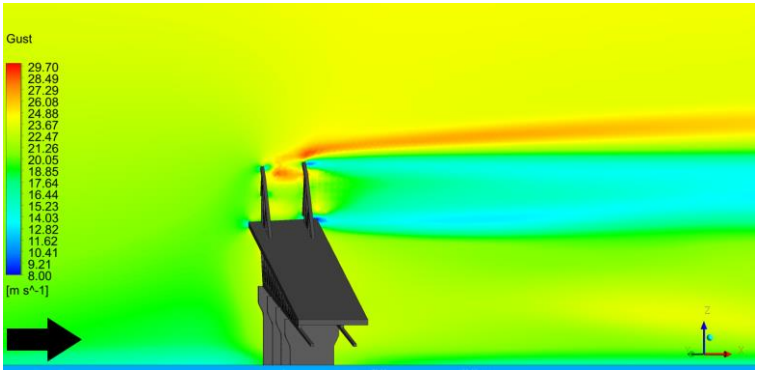

Figure 6. Estimated gust wind speed (Eqs. 4-6) on a cross-sectional plane of the harbour.

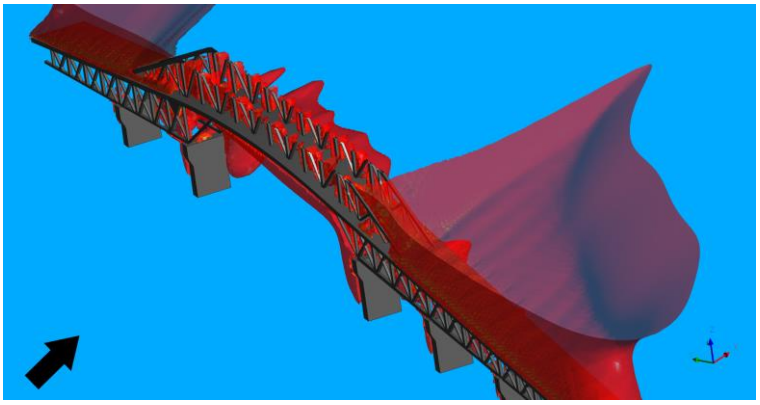

Figure 7. Velocity iso-surface showing the locations where the velocity is 18 m/s. The top arch is removed from the visualisation to better show the iso-surface on the road.

4. Conclusions

The study investigated the feasibility of coupling a very high-resolution NWP model over Auckland, New Zealand, with grid size of 333 m, to a CFD model. The primary aim was to assess the 333-m model's performance during this high-wind event in Auckland on 18 September 2020, and also to carry out a CFD simulation of the airflow around the Auckland Harbour using a RANS method. The CFD simulations demonstrated that the bridge influences the incoming airflow such that the mean speed on the road can increase by up to 1.20 compared with the undisturbed upstream flow. In addition, while underestimating the observed mean and gust wind speeds at the bridge, coupling the 333-m NWP and CFD model shows promise for better predicting extreme wind events, since the CFD provides information on local speed-ups, which is what is missing from an NWP model that does not see the finer structures.

Gaining a better understanding of the detailed airflow patterns over the Auckland Harbour bridge can aid developing a warning system to avoid events like the one happened on 18 September 2020. More work is underway to use large eddy simulation (LES) instead of RANS to study the flow pattern in more detail as well as advancing our capability in coupling NWP outputs to CFD simulations.

Acknowledgment

This work was supported in part by the Weather and Wildfire Theme of the Resilience to Natures' challenge funded by New Zealand's Ministry of Business Innovation and employment as well as by NIWA through that Climate and Forecasting program of NIWA's Strategic Science Investment Fund. The authors wish to acknowledge the use of New Zealand eScience Infrastructure (NeSI) high performance computing facilities (https://www.nesi.org.nz).

References

Baik, J.-J., Park, S.-B., Kim, J.-J., 2009. Urban Flow and Dispersion Simulation Using a CFD Model Coupled to a Mesoscale Model. *J. Appl. Meteorol. Clim.* 48:1667-1681. DOI: 10.1175/2009jamc2066.1

Boutle, I.A., Finnenkoetter, A., Lock, A.P., Wells, H., 2016. The London Model: forecasting fog at 333m resolution. *Q. J. R. Meteorol. Soc.* 142:360-371. DOI: 10.1002/qj.2656

Bush, M., Allen, T., Bain, C., Boutle, I., Edwards, J., Finnenkoetter, A., Franklin, C., Hanley, K., Lean, H., Lock, A., Manners, J., Mittermaier, M., Morcrette, C., North, R., Petch, J., Short, C., Vosper, S., Walters, D., Webster, S., Weeks, M., Wilkinson, J., Wood, N., Zerroukat, M., 2020. The first Met Office Unified Model–JULES Regional Atmosphere and Land configuration, RAL1. *Geosci. Model Dev.* 13:1999-2029.

Durán, P., Meiβner, C., Casso, P., 2020. A new meso-microscale coupled modelling framework for wind resource assessment: A validation study. *Renew. Energ.* 160:538-554. DOI: 10.1016/j.renene.2020.06.074

Holmes, J.D., 2015. "Wind loading of structures", 3rd Edition. Taylor & Francis Group.

Kadaverugu, R., Sharma, A., Matli, C., Biniwale, R., 2019. High Resolution Urban Air Quality Modeling by Coupling CFD and Mesoscale Models: a Review. *Asia-Pacific J. Atmos. Sci.* 55:539-556.

Liu, Y.S., Miao, S.G., Zhang, C.L., Cui, G.X., Zhang, Z.S., 2012. Study on micro-atmospheric environment by coupling large eddy simulation with mesoscale model. *J. Wind Eng. Ind. Aerodyn.* 107-108:106-117.

Piroozmand, P., Mussetti, G., Allegrini, J., Mohammadi, M.H., Akrami, E., Carmeliet, J., 2020. Coupled CFD framework with mesoscale urban climate model: Application to microscale urban flows with weak synoptic forcing. *J. Wind Eng. Ind. Aerodyn.* 197:104059. DOI: 10.1016/j.jweia.2019.104059

Popiolek, Z., 2008. Estimation of Mean Speed and Standard Deviation from CFD Prediction. *Archit. Civil Eng. Environ.* 1:141-146.

Richards, P.J., Norris, S.E., 2015. Appropriate boundary conditions for a pressure driven boundary layer. *J. Wind Eng. Ind. Aerodyn.* 142:43-52. DOI: 10.1016/j.jweia.2015.03.003

Safaei Pirooz, A.A., Flay, R.G.J., 2018. Comparison of Speed-Up Over Hills Derived from Wind-Tunnel Experiments, Wind-Loading Standards, and Numerical Modelling. *Boundary-Layer Meteorol.* 168:213-246. DOI: 10.1007/s10546-018-0350-x

Safaei Pirooz, A.A., Flay, R.G.J., Minola, L., Azorin-Molina, C., Chen, D., 2020. Effects of sensor response and moving average filter duration on maximum wind gust measurements. *J. Wind Eng. Ind. Aerodyn.* 206, 104354. DOI: 10.1016/j.jweia.2020.104354

Stuff, 2018. Auckland Harbour Bridge chaos: Tipped truck causes gridlock on motorways. https://www.stuff.co.nz/national/300110727/auckland-harbour-bridge-chaos-tipped-truck-causes-gridlock-on-motorways

Walters, D., Boutle, I., Brooks, M., Melvin, T., Stratton, R., Vosper, S., Wells, H., Williams, K., Wood,, N., A., T., Bushell, A., Copsey, D., Earnshaw, P., Edwards, J., Gross, M., Hardiman, S., Harris, C.,, Heming, J., Klingaman, N., Levine, R., Manners, J., Martin, G., Milton, S., Mittermaier, M., Morcrette,, C., R., T., Roberts, M., Sanchez, C., Selwood, P., Stirling, A., Smith, C., Suri, D., Tennant, W.,, Vidale, P.L., Wilkinson, J., Willett, M., Woolnough, S., and Xavier, P. , 2017. The Met Office Unified Model Global Atmosphere 6.0/6.1 and JULES Global Land 6.0/6.1 configurations. *Geosci. Model Dev.* 10:1487-1520. DOI: 10.5194/gmd-10-1487-2017